Pharm Res (2012) 29:3040–3052
DOI 10.1007/s11095-012-0726-4

RESEARCH PAPER

Novel Tubulin Polymerization Inhibitors Overcome Multidrug Resistance and Reduce Melanoma Lung Metastasis

Zhao Wang • Jianjun Chen • Jin Wang • Sunjoo Ahn • Chien-Ming Li • Yan Lu • Vivian S. Loveless • James T. Dalton • Duane D. Miller • Wei Li

Received: 17 October 2011 / Accepted: 27 February 2012 / Published online: 13 March 2012

ABSTRACT

Purpose To evaluate abilities of 2-*a*ryl-4-*b*enzoyl-*i*midazoles (ABI) to overcome multidrug resistance (MDR), define their cellular target, and assess *in vivo* antimelanoma efficacy.

Methods MDR cell lines that overexpressed P-glycoprotein, MDR-associated proteins, and breast cancer resistance protein were used to evaluate ABI ability to overcome MDR. Cell cycle analysis, molecular modeling, and microtubule imaging were used to define ABI cellular target. SHO mice bearing A375 human melanoma xenograft were used to evaluate ABI *in vivo* antitumor activity. B16-F10/C57BL mouse melanoma lung metastasis model was used to test ABI efficacy to inhibit tumor lung metastasis.

Results ABIs showed similar potency to MDR cells compared to matching parent cells. ABIs were identified to target tubulin on the colchicine binding site. After 31 days of treatment, ABI-288 dosed at 25 mg/kg inhibited melanoma tumor growth by 69%; dacarbazine at 60 mg/kg inhibited growth by 52%. ABI-274 dosed at 25 mg/kg showed better lung metastasis inhibition than dacarbazine at 60 mg/kg.

Conclusions This new class of antimitotic compounds can overcome several clinically important drug resistant mechanisms *in vitro* and are effective in inhibiting melanoma lung metastasis *in vivo*, supporting their further development.

KEY WORDS 2-*a*ryl-4-*b*enzoyl-*i*midazoles (ABI) · antimelanoma · melanoma lung metastasis · multidrug resistance · tubulin polymerization inhibitor

ABBREVIATIONS

μM	micromolar per liter
ABI	2-*a*ryl-4-*b*enzoyl-*i*midazole compounds
BCRP	breast cancer resistance protein
DAMA-colchicine	N-deacetyl-N-(2-mercaptoacetyl)-colchicine
DMSO	dimethyl sulphoxide
DTIC	dacarbazine
FBS	fetal bovine serum
HMEC	human microvascular endothelial cells
MDR	multidrug resistant
MRP	MDR associated proteins
MTD	maximum tolerable dose
nM	nanomolar per liter
SAR	structure-activity relationship
SCID	severe combined immunodeficiency
SHO mice	double homozygous SCID hairless outbreed mice
SMART	substituted methoxylbenzoyl-aryl-thiazole
SPA	scintillation proximity assay

Electronic supplementary material The online version of this article (doi:10.1007/s11095-012-0726-4) contains supplementary material, which is available to authorized users.

Z. Wang • J. Chen • J. Wang • Y. Lu • V. S. Loveless • D. D. Miller • W. Li (✉)
Department of Pharmaceutical Sciences
University of Tennessee
Health Science Center
847 Monroe Ave., Room 327
Memphis, Tennessee 38163, USA
e-mail: wli@uthsc.edu

S. Ahn • C.-M. Li • J. T. Dalton
Preclinical Research and Development Department GTx, Inc.
Memphis, Tennessee, USA

Present Address:
Z. Wang
Frontage Laboratories, Inc.
Exton, Pennsylvania, USA

SRB	sulforhodamine B
TGI	tumor growth inhibition

INTRODUCTION

Metastatic melanoma is the most dangerous type of skin cancer, accounting for 75 % of skin cancer deaths (1). Patients with advanced melanoma with dissemination to distant sites and visceral organs have a very poor prognosis, with a median survival time of 6 months and a 5-year survival rate of less than 5 % (1). Before 2011, the Food and Drug Administration (FDA) had approved only one small-molecule drug for metastatic melanoma, dacarbazine (DTIC), an alkylating agent, but it provides less than 5 % complete remission (2). Neither combinations of DTIC and other chemotherapy drugs (e.g., cisplatin, vinblastine, and carmustine) nor adding interferon-α2b to DTIC has shown a survival advantage over DTIC alone(3). Clinical trials with antibodies or vaccines to treat melanoma have also failed to demonstrate satisfactory efficacy (4).

The year 2011 marks a fruitful year for melanoma research. The FDA approved three drugs for advanced melanoma treatment: ipilimumab (an anticytotoxic T lymphocyte antigen-4 monoclonal antibody), vemurafenib (a selective BRAF inhibitor), and pegylated interferon-α2b for adjuvant setting usage (5). However, there are still significant limitations for melanoma treatment. Ipilimumab only prolonged the survival time for metastatic melanoma patient from an average of 6.5 months to an average of 10 months. This treatment also has been associated with strong immunological adverse effects; severe to fatal autoimmune reactions were seen in 12.9 % of patients treated with ipilimumab in a clinical trial that enrolled 676 melanoma patients (6). Vemurafenib is not effective for melanoma patients with wide type Braf, and confirmation of $BRAF^{V600E}$ mutation-positive melanoma using an FDA-approved test is required before treatment with vemurafenib. This treatment also only prolonged the median survival time for advanced melanoma patients 2~3 months (5). More importantly, despite the high initial response rate for patients with $BRAF^{V600E}$ mutation to vemurafenib, virtually all the patients developed primary or acquired resistance to this drug (7). With the rapidly rising incidents of this disease

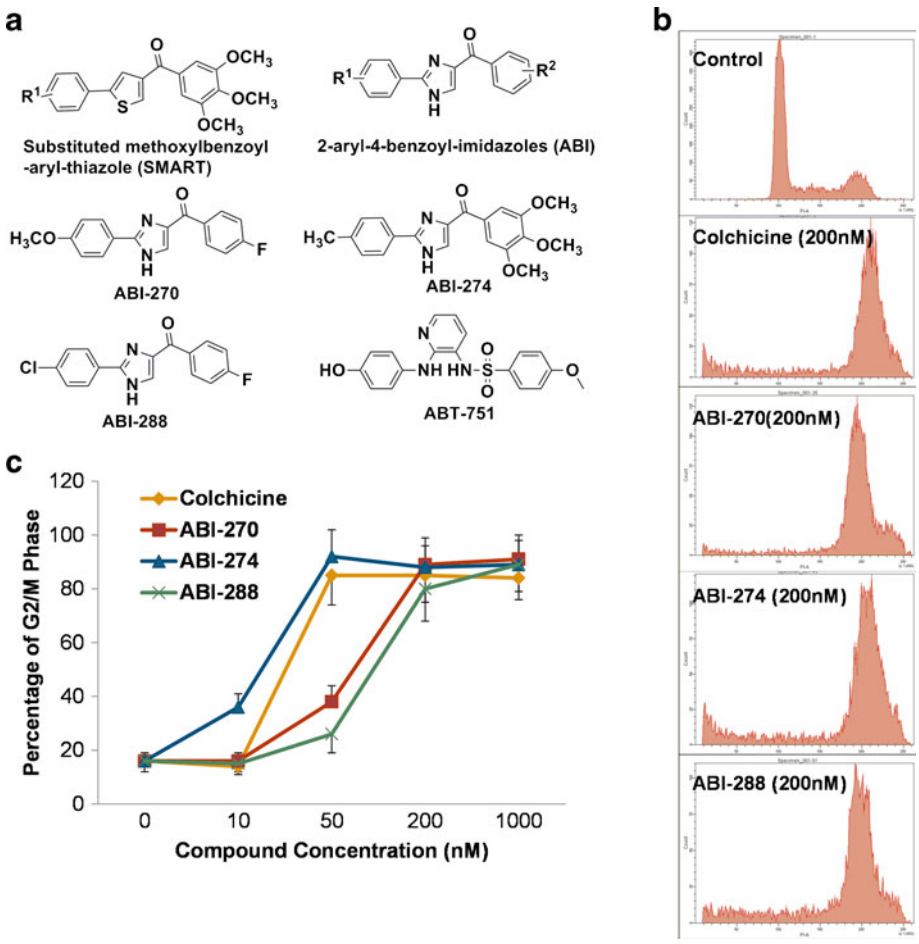

Fig. 1 Chemical structures of ABIs and cell cycle arrest upon ABI treatment. (**a**) General structures of SMART and ABIs, along with structures of ABI-270, -274, -288 m and ABT-751. (**b**) Cell cycle analysis showed that ABIs and colchicine arrest A375 cells in the G2/M phase after 24-h incubation. (**c**) Quantification of cell cycle analysis.

and the high resistance to current therapeutic agents, developing more effective drugs for melanoma is very important.

We previously reported the discovery of substituted methoxybenzoyl-aryl-thiazoles (SMART) (8) and the chemistry of the more aqueous soluble analogs, 2-aryl-4-benzoyl-imidazoles (ABI) (9). The general structures of SMARTs and ABIs are shown in Fig. 1a. Here we report detailed biological studies for ABIs by using three representative compounds (ABI-270, ABI-274, and ABI-288, see Fig. 1a) to clearly define their cellular target, assess their ability to overcome a number of clinically important drug-resistant mechanisms, and evaluate *in vivo* efficacy against melanoma tumors and their lung metastasis.

MATERIALS AND METHODS

Compounds and Reagents

ABI-270, ABI-274, ABI-288, and ABT-751 (a drug in clinical development by Abbott Labs (10), structure and synthesis shown in Supplementary Material, Figure S1) were synthesized in our lab. Paclitaxel, vinblastine, colchicine, dimethyl sulfoxide (DMSO), SN-38, PEG300, and Tween 80 were purchased from Sigma-Aldrich (St. Louis, MO). Captex 200 was obtained from ABITEC Corporation (Paris, IL). CellTiter 96 AQueous One Solution Reagent was purchased from Promega Corporation (Madison, WI). DTIC was obtained from APP Pharmaceuticals, LLC (Schaumburg, IL).

Cell Culture

Human A375 cells, mouse B16 melanoma cells, and human microvascular endothelial cells (HMEC) were purchased from American Type Culture Collection (ATCC, Manassas, VA). HMEC cells can proliferate and migrate to form tube-like structures, mimicking *in vivo* angiogenesis process (11). Human metastatic WM-164 cells isolated from a patient with metastatic melanoma were a gift from Dr. Meenhard Herlyn (Wistar Institute, Philadelphia, PA). The P-gp overexpressing multidrug-resistant cell line MDA-MB-435/LCC6MDR1 and the matching sensitive parent cell line were kindly provided by Dr. Robert Clarke (Georgetown University, Washington, DC). Human ovarian cell line OVCAR-8 and its adriamycin-resistant cell line that overexpresses P-gp, NCI/ADR-RES, were obtained from the National Cancer Institute (Frederick, MD). PcDNA3.1 vector was purchased from Invitrogen (Carlsbad, CA). PcDNA3.1 vectors containing human MRP1 and MRP2 cDNAs were obtained from Dr. Susan P. C. Cole (Department of Pharmacology & Toxicology, Queen's University, Kingston, Ontario Canada) and transfected into HEK-293 cells in 2007 (12). HEK293-482R2 is a breast cancer resistance protein (BCRP) overexpressing cell line and was kindly provided by Dr. Duxin Sun in 2007 (College of Pharmacy, The Ohio State University, Columbus, OH). HEK293-482R2 was transfected with either empty pcDNA3 vector (Invitrogen, Carlsbad, CA, USA) containing full-length ABCG2 coding an arginine for amino-acid 482. A375MA2 cells were obtained from Drs. Lei Xu and Richard Hynes (Howard Hughes Medical Institute, Massachusetts Institute of Technology, Cambridge, CA). A375MA2 cells were derived by culturing A375 cells isolated from the lung metastasis of A375 melanoma tumor in nude mice for two times. A375, A375MA2, B16-F1, B16-F10, WM-164, MDA-MB-435, MDA-MB-435/LCC6MDR1, and HEK-293 cells were cultured in DMEM (Mediatech, Inc., Manassas, VA), supplemented with 10 % fetal bovine serum (FBS) (Atlanta Biologicals, Lawrenceville, GA), 1 % antibiotic/antimycotic mixture (Sigma-Aldrich, St. Louis, MO), and bovine insulin (5 μg/ml) (Sigma-Aldrich, St. Louis, MO). HMECs were cultured in EBM-2 medium (Lonza, Walkersville, MD) containing 10 % FBS, 0.1 ng/ml epidermal growth factor, and 1 μg/ml hydrocortisone. OVCAR-8 and NCI/ADR-RES cells were maintained in RPMI-1640 medium (Thermo Scientific, Rockford, IL) with 2 mM L-glutamine and 10 % FBS. All cell lines were authenticated by Research Animal Diagnostic Laboratory (Columbia, MO).

Growth Inhibition Assay

The cytotoxic or antiproliferative activity of test compounds was investigated in several cell lines by using the sulforhodamine B (SRB) assay. Cultured cells were plated in 96-well plates and incubated with titration of the test compounds. The cells were stained with SRB after 96 h treatment, and the optical density of stained cells was measured at 540 nm on a microplate reader (BioTek Instruments, Winooski, VT) (13).

P-gp ATPase Assay

P-gp ATPase assay was conducted using the Pgp-Glo™ Assay System (Promega, Madison, WI) according to the manufacturer's protocol. Na_3VO_4 (100 μM), a selective inhibitor of P-gp without P-gp ATPase activity, and verapamil (200 μM), a known P-gp substrate with the ATPase activity stimulation, were used as control substrates as provided by Pgp-Glo™ Assay System. 0.5 % DMSO was used as vehicle control. Compound ABI-270, -274, and -288 were tested at 10, 100, and 1000 nM. Briefly, after adding tested compounds, ATP (5 mM per reaction) was added and incubated with P-gp membrane (25 μg per reaction) at 37 °C for 45 min. Then the P-gp ATPase reactions were stopped by removing from 37 °C. The remaining unmetabolized ATP was detected as a luciferase-generated luminescent signal detected using a

Synergy 4 Hybrid Multi-Mode Reader (BioTek Instruments, Winooski, VT). All tests were done in triplicates.

Cell Cycle Analysis

Flow cytometry analysis was performed as described elsewhere (14) to study cell cycle phase distribution. A375 cells were cultured in 10-cm tissue culture dishes until confluence was 80 % and were treated with 0, 10, 50, 200, and 1000 nM of colchicine, ABI-274, and ABI-288 for 24 h in growth media. Cellular DNA was stained with PBS containing 50 μg/ml propidium iodide and 100 μg/ml RNase A. The cell cycle was determined using a BD LSR-II cytometer (BD Biosciences, San Jose, CA) with 10,000 cells scored. Data were analyzed and graphs were prepared using the Modfit 2.0 program (Verity Software House, Topsham, ME).

Molecular Modeling

We selected the crystal structure of N-deacetyl-N-(2-mercaptoacetyl)-colchicine (DAMA-colchicine) in tubulin complex (PDB code: 1SA0), which has been most widely used for modeling approaches (15). We used Schrodinger Molecular Modeling Suite (Schrodinger LLC, New York, NY) for the docking practice. ABIs were built and prepared using the Ligprep module, and they were docked into the colchicine binding site using the Glide module in the Schrodinger Suite. The best docking complexes were subject to restricted molecular dynamics to release any strains by using Macromodel module with OPLS-2005 force field. The ligand and its surrounding residues within 15 Å were allowed to move freely, while residues outside the 15-Å radius were kept rigid.

Microtubule Imaging Using Immunofluorescence Microscopy

Cellomics Cytoskeleton rearrangement kit (Thermo Scientific, Rockford, IL) was used to study the interactions of ABIs with tubulin in cells. WM-164 melanoma cells were treated with each compound for 18 h in duplicate using a collagen-coated 96-well plate (Becton Dickinson Labware, Bedford, MA). Cells were fixed with 4 % paraformaldehyde (Thermo Scientific, Rockford, IL) and permeabilized using permeabilization buffer supplied with the kit. Primary antibody for tubulin and fluorescence-labeled secondary antibody were subsequently added to the cells. Cell nuclei were stained by DAPI. Whole cell stain green was also applied to all cells. Images were acquired with an Olympus IX71 inverted fluorescence microscope (Olympus Corp., Tokyo, Japan) with overlays from separate images of tubulin (red), nuclei (blue), and whole cells (green). For comparison, we also included paclitaxel, colchicine, and ABT-751, along with ABI compounds.

Colony Formation Assay in Soft Agar

B16-F1 melanoma cells were plated at a colony-forming density (2000 cells per well in 6-well plates) on top of 0.8 % base agar. Cells were grown in 0.4 % agar together with DMEM medium supplemented with FBS at 37 °C (16). Cells were treated with ABI-274 and ABI-288 at different concentrations (20, 100, and 500 nM). Compounds were added to the media from 1-mM DMSO stock solutions, and a corresponding dilution of DMSO was used as control. Cells were incubated for 14 days. Plates were photographed, and the number of colonies was measured by Artek 880 Automated Colony Counter (Artek Systems Corporation, Farmingdale, NY).

In Vitro Capillary Network Formation on Matrigel

200 μl of 5.25 mg/ml Matrigel (BD Biosciences, Pont de Claix, France) were added to 48-well plates and allowed to solidify for 1 h at 37 °C. Each well was seeded with 7×10^4 HMEC and cultured in EBM-2 medium containing various concentrations of ABI-288 (30, 100, 300 nM, 1, 3, 10, and 30 μM) or 0.1 % DMSO (v/v) for 4 h. Photographs from five randomly chosen fields of each condition were taken using an IX71 microscope (Olympus, Tokyo, Japan) (17,18).

In Vivo Antitumor Study on Xenograft Model

We first estimated the acute maximum tolerable dose (MTD) for each of the three ABI analogs formulated in PEG300. Progressively increasing injection doses via i.p. route to C57BL/6 mice (two mice in a group) determined the estimated MTD to be 150 mg/kg with one-time injection. To ensure a safety margin during the repeated treatment, we scaled down the dose to 25 mg/kg in the animal experiments.

Double homozygous severe combined immunodeficiency (SCID) hairless outbreed (SHO) mice, 6–8 weeks old, were provided by Charles River Laboratories International, Inc. (Wilmington, MA). Logarithmic growth phase A375 (5×107 per ml) cells were prepared in phenyl red-free, FBS-free DMEM media and mixed at 1:1 ratio with Matrigel. Tumors were established by injecting 100 μl of this mixture subcutaneously in the right dorsal flank of each mouse (2.5×10^6 cells). When the tumor reached a mean size of 100 ~ 150 mm^3, mice were randomized into three groups and treatments were started. ABIs were formulated with Tween80/Captex200 (80/20). ABI compound at 25 mg/kg was used with i.p. injection of 30 μl of compound solution once daily for 31 days. The control group was given only a vehicle solution injection at the same frequency. DTIC was reconstituted with sterile water, and 100 μl of this solution was administrated via i.p. injection once daily for 31 days. Tumor volume was measured three times a week with a digital caliper and calculated by using the formula $a\times b^2\times0.5$, where a and b represented the

larger and smaller diameters, respectively (19). Data were expressed as mean ± SD for each group and plotted as a function of time. Tumor growth inhibition (TGI) at the conclusion of the experiments was calculated from the formula 100-100*[(*T-T0*)/(*C-C0*)] where *T* represented mean tumor volume of a treated group on a specific day, *T0* represented mean tumor volume of the same group on the first day of treatment, *C* represented mean tumor volume of a control on a specific day, and *C0* represented mean tumor volume of the same group on the first day of treatment (14,20). Animal activity and body weight were monitored during the entire experiment period to assess potential acute toxicity.

In Vivo Melanoma Cells Lung Metastasis Study

C57BL/6 mice from Charles River Laboratories International, Inc., age 7–8 weeks old, were used to study the inhibition effect of ABIs in lung metastasis of melanoma cells. The logarithmic growth phase B16-F10 melanoma cells (75,000 cells in 100 μL PBS buffer per mouse) were injected via the lateral tail vein. The treatment started from the 7^{th} day after the inoculation. Our test runs and literature reports indicated that 3 weeks after injection is the optimal window to examine tumor nodules in the lung in this experimental metastasis model. The 1-week delay of treatment ensured lung metastasis before compound treatment. Compared with the procedures reported in the literature in which compound treatment started 15 ~ 30 min after melanoma cell injection, we believed that delaying treatment by 1 week allowed tumors to have sufficient time to metastasize to the lungs, a situation that is likely to be more clinically relevant. ABIs (25 mg/kg) were formulated with PEG300 while DTIC (60 mg/kg) was reconstituted with sterile water (21). All the treatment solutions were kept in the same volume (100 μl) and administered through i.p. injection for 2 weeks, 5 days a week. Vehicle control group was treated with i.p. injection of 100 μL PEG300. Mice were sacrificed after 15 days of treatment, and the lungs were separated and expanded with 10 % formalin buffer. The number of lung metastasis nodules was noted. Animal activity and body weight were monitored during the entire experiment period to assess acute toxicity.

Data Analysis

Data were analyzed using Prism Software (GraphPad Software, Inc., San Diego, CA). The statistical significance ($P < 0.05$) was evaluated by repeated measures two-way ANOVA for xenograft study and one-way ANOVA for melanoma lung metastasis study. Dunnett's multiple comparison test was done after ANOVA analysis.

RESULTS

ABIs Inhibit Melanoma Cell Proliferation with High Potency and Can Effectively Overcome Multidrug Resistance in Cancer Cells

As we reported earlier, ABIs have excellent antiproliferative activity (IC_{50} values less than 100 nM) against a variety of cancer cell lines (9). We compared the activity of ABIs with paclitaxel, vinblastine, colchicine, and ABT-751 in Table I. ABIs showed excellent potency on all three melanoma cell lines with IC_{50} values less than 80 nM. They have comparable potency with paclitaxel or colchicine and are significantly more potent than ABT-751. More importantly, ABIs showed similar, or in some case higher, potency against more metastatic melanoma cells A375MA2 (Table I). These cells were derived by culturing A375 cells isolated from in the lung metastasis of A375 melanoma tumor in nude mice for two times and showed dramatic increased lung metastatic ability after this series of culturing selection (22). Taken together, these results suggested that ABIs strongly inhibit growth of metastatic melanoma cells.

Table I also summarizes results when compounds were tested on multidrug resistant (MDR) cell lines and the matching parent cell lines. Some representative dose response curves are shown in Figure S2. P-gp overexpressed cells like MDA-MB-435/LCCMDR1 and NCI/ADR-RES were 28- to 511-fold more resistant to colchicine, paclitaxel, and vinblastine. High MDR-associated protein (MRP) expression cells were 3 to 6 times more resistant to paclitaxel and vinblastine. SN-38 was used to verify the drug resistance effect of BCRP-transfected cell line HEK293-482R2. The resistance index (calculated by dividing IC_{50} values of the resistant cell subline by that of the matching parental cell line) of SN-38 on cells transfected with the BCRP gene was 41. In contrast, all tested ABIs showed very similar potency to MDR cells compared with the matching parent cells, strongly suggesting that they are not affected by the over-expression of MDR transporters in cells and thus are promising candidates for treating MDR melanoma.

ABIs Do Not Affect P-gp (MDR1) ATPase Activity

To further test whether ABIs interact with P-gp, we tested their effects on P-gp ATPase activity using commercially available commercial kit. Results of this assay were shown in Fig. 2a and b. In Fig. 2a, the decrease in luminescence of vehicle treated samples compared to Na_3VO_4 treated samples represents basal P-gp ATPase activity. The decrease in luminescence of verapamil treated samples compared to Na_3VO_4 treated samples represents verapamil-stimulated P-gp ATPase activity. This verified the assay system worked well. The change of luminescence was replotted in Fig. 2b to illustrate

Table 1 ABIs Showed Excellent Potency Against All Tested Melanoma Cell Lines Including Highly Metastatic and Multidrug Resistant Cell Lines

	$IC_{50} \pm SEM$ (nmol/L) ($n=3$)							
	ABI-270	ABI-274	ABI-288	Paclitaxel	Vinblastine	Colchicine	ABT-751	SN-38
A375	31 ± 5	9 ± 2	52 ± 4	12 ± 3	1 ± 0.1	20 ± 3	685 ± 108	ND
A375MA2	44 ± 5	8 ± 1	55 ± 4	8 ± 1	1 ± 0.2	18 ± 2	265 ± 36	ND
B16-F1	63 ± 7	46 ± 5	73 ± 6	17 ± 2	5 ± 1	29 ± 5	2127 ± 351	ND
WM-164	28 ± 3	8 ± 2	74 ± 9	18 ± 3	0.6 ± 0.1	10 ± 2	661 ± 56	ND
MDR1 (P-gp)								
MDA-MB-435[a]	24 ± 2	5 ± 1	41 ± 2	4 ± 1	0.4 ± 0.1	10 ± 1	417 ± 23	ND
MDA-MB-435/LCC6MDR1	30 ± 4 (1)	11 ± 2 (2)	38 ± 2 (1)	277 ± 4 (69)	11 ± 1 (28)	658 ± 50 (66)	577 ± 31 (1)	ND
OVCAR-8[a]	25 ± 2	11 ± 1	45 ± 2	10 ± 0.2	2 ± 0.1	12 ± 1	785 ± 17	2 ± 0.2
NCI/ADR-RES	13 ± 1 (0.5)	5 ± 0.1 (0.5)	20 ± 6 (0.4)	5109 ± 170 (511)	570 ± 84 (285)	737 ± 51 (61)	864 ± 42 (1)	10 ± 1 (5)
MRP								
HEK293 -pcDNA3.1[a]	12 ± 2	9 ± 1	54 ± 0.3	9 ± 0.3	5 ± 0.1	3 ± 0.4	645 ± 153	3 ± 0.4
HEK293-MRP1	16 ± 2 (1)	8 ± 1 (0.9)	33 ± 7 (0.6)	30 ± 3 (3)	24 ± 1 (5)	5 ± 0.1 (2)	717 ± 28 (1)	9 ± 0.04 (3)
HEK293-MRP2	14 ± 4 (1)	8 ± 0.3 (0.9)	39 ± 12 (0.7)	37 ± 2 (4)	28 ± 2 (6)	3 ± 0.3 (1)	747 ± 7 (1)	7 ± 0.1 (2)
BCRP								
HEK293-482R2	17 ± 1 (1)	8 ± 1 (0.9)	23 ± 3 (0.4)	50 ± 1 (6)	25 ± 1 (5)	5 ± 0.1 (2)	653 ± 72 (1)	123 ± 28 (41)

[a] parental cell line to drug resistant cell subline; MDR1 were overexpressed in MDA-MB-435/LCC6MDR1 and NCI/ADR-RES; MRP1, MRP2 and BCRP were overexpressed in HEK293-MRP1, HEK293-MRP2, and HEK293-482R2. The resistance indexes (numbers in the parenthesis) were calculated by dividing IC_{50} values on the resistant cell subline by that of the matching parental cell line. Abbreviations: N/A, not applicable since they bind to tubulin at different sites. ND, not determined. For completeness, we also included few *in vitro* data that were reported in our previous paper [9] in this table

the stimulation or inhibition of P-gp ATPase activity by compounds treatment. Y values (change in luminescence) are the difference between Na_3VO_4 treated samples and testing compounds treated samples. We did statistical analysis to compare groups in Fig. 2b using Prism software. Dunnett's multiple comparison test after ANOVA analysis gave an overall P value of less than 0.05. For each individual comparison with vehicle control, only verapamil treated wells has $P<0.05$. All other comparison gave P values larger than 0.05. There is no statistical difference between vehicle treated wells and ABI compounds treated wells at all tested concentration. These results indicated that ABI compounds do not affect P-gp ATPase activity, suggesting that they were neither stimulator, nor inhibitor for P-gp ATPase.

ABIs Inhibit Tubulin Polymerization by Binding to the Colchicine Site in Tubulin

Our previous preliminary studies suggested that ABIs may target tubulin polymerization by binding to the colchicine binding site (9). We have expanded those studies significantly and performed additional experiments to confirm this mechanism of action summarized below. We first determined the effects of ABIs on cell cycle progression. We tested ABI-270, -274, -288, and colchicine (positive control) on A375 melanoma cells at four concentrations (10, 50, 200, and 1000 nM) (Fig. 1b and c; additional results can be found in Supplementary Material, Figure S3). For vehicle controls, 16 % of A375 cells were distributed in the G2/M phase. For the colchicine-treated group, as concentration increased from 10 nM to 50 nM, the percentage of cells distributed in the G2/M phase increased from 14 % to 85 %. ABIs showed similar effects in arresting cells in the G2/M phase in a dose-dependent manner. The potency of the different concentrations in arresting cells in the G2/M phase positively qualitatively correlated with *in vitro* activity.

We next expanded *in vitro* tubulin polymerization assays and competitive binding assay in tubulin with [^{3}H]colchicine for all three ABI-compounds. The results are similar to what we have reported for one of these compounds in our previous study (9). The complete results are shown in Supplementary Material, Figures S4 and S5.

Finally, using molecular modeling techniques, we tried to understand the potential binding pose of ABIs to the colchicine binding site on tubulin using the crystal structure of tubulin in complex with DAMA-colchicine (PDB code: 1SA0) (23). ABI-270, -274, and -288 showed excellent binding to the colchicine site. As an example, the binding mode of ABI-288 (stick model) is shown in Fig. 3a. For comparison, we also displayed the native ligand DAMA-colchicine as a wire model in the α/β-tubulin heterodimer. The overall structure of ABI-288 and DAMA-colchicine overlapped very well. The *p*-fluoro phenyl moiety overlaps with the trimethoxyphenyl moiety, which is interacting with the T7 loop in the β-subunit. Similarly, the *p*-chloro phenyl moiety occupies the other side of the pocket where the seven-member ring of the DAMA-colchicine is, with the chlorine atom occupying the pocket where the methoxy moiety interacts.

ABIs Prevent Microtubule Formation

To further confirm that ABIs interact with tubulin in melanoma cells, we examined microtubule arrangement in WM-164 cells upon treatment with different compounds (Fig. 3b). These images clearly showed that all five tested compounds resulted in cytoskeleton rearrangement. There was a significant difference between paclitaxel and the other four compounds (colchicine, ABT-751, ABI-274, and ABI-

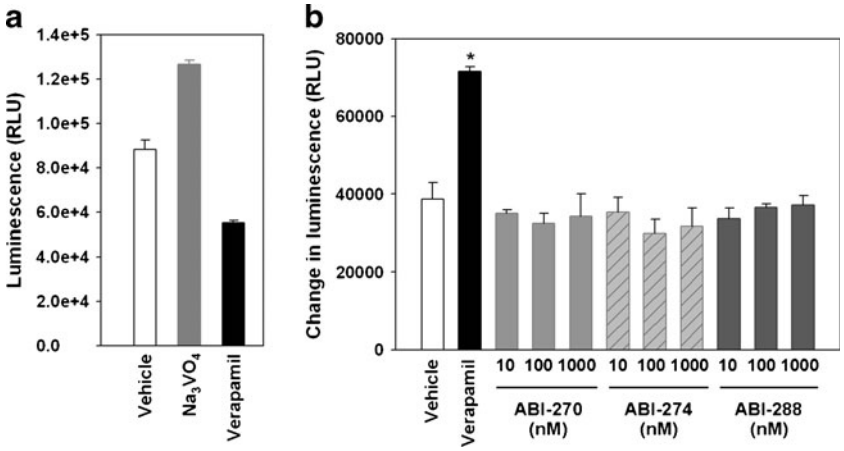

Fig. 2 Effects of ABI compounds on P-gp ATPase activity. (**a**) Positive, negative and vehicle control for P-gp ATPase activity. The decrease in luminescence of vehicle treated samples compared to Na_3VO_4 treated samples represents basal P-gp ATPase activity. The decrease in luminescence of verapamil treated samples compared to Na_3VO_4 treated samples represents verapamil-stimulated P-gp ATPase activity. (**b**) Change in luminescence compared to Na_3VO_4 treated samples. ABI compounds showed similar effect as vehicle control on P-gp ATPase activity, indicate they are not substrate for P-gp. * $P<0.05$; column, mean of three replication; bar, SD.

288). Treatment with paclitaxel resulted in a stabilization of microtubules around the nuclei compared with controls, consistent with its mechanisms of action for inhibiting tubulin polymerization by stabilizing microtubules. On the contrary, treatment with colchicine, ABT-751, ABI-274, and ABI-288 had similar effects on microtubules and resulted in microtubule fragmentation, consistent with their common mechanism of action for inhibiting tubulin polymerization by destabilizing microtubules. The higher concentration used for ABT-751 is due to its lower *in vitro* potency compared with other compounds.

ABIs Inhibit Melanoma Colony Formation in Soft Agar

Colony formation assay has been generally used to predict the therapeutic efficacy of a drug to solid tumors (24). We tested the ability of ABI-270, -274, and -288 to inhibit melanoma colony formation in soft agar at three concentrations (20, 100, and 500 nM). Four representative photos are shown in Fig. 4a; additional photos can be found in Supplementary Material, Figure S6. Quantified results are shown in Fig. 4b. After 14 days of incubation, 130 detectable colonies (diameter larger than 100 μm) were formed in controls. ABI-274 effectively inhibited melanoma colony formation at the lowest tested concentration, 20 nM ($P<0.05$), compared with control). ABI-288 showed effective inhibition at 100 nM. All tested compounds showed complete inhibition of colony formation at 0.5 μM. Dunnett's multiple comparison tests after ANOVA gave an overall P value of less than 0.0001, suggesting the means of the seven compared groups are statistically different. For Dunnett's test, at significance level of 0.05, only the group means of ABI-270 and -288 at 20 nM were not statistically different from control.

ABIs Inhibit *In Vitro* Capillary Network Formation on Matrigel

Many tubulin target agents including paclitaxel and colchicine have strong antiangiogenesis effects (25,26). We hypothesized that ABIs also possess such an effect because they also target tubulin polymerization. To test this hypothesis, we evaluated the effect of ABI-288 on the formation of capillary-like network by HMEC cells plated on Matrigel. Matrigel provides endothelial cells a supporting environment for differentiation into an extensive and enclosed capillary-like network. The tube structure was destructed and displayed an incomplete tube network when incubated with ABI-288 at 30 nM compared with control (Fig. 4c). ABI-288 at a concentration of 100 nM and above caused complete inhibition of capillary network formation. Because this inhibition effect occurred within 4 h and at a very low concentration (30 nM), this effect was not the result of the antiproliferative activity of the compound. This experiment indicated that ABIs have strong antiangiogenesis effect.

ABIs Inhibited Melanoma Tumor Growth *In Vivo*

ABIs' *in vivo* antitumor efficacy was first tested on a human melanoma xenograft model in SHO mice. Compound ABI-288 was chosen because it was expected to be more metabolically stable due to the absence of the trimethoxyphenyl group (27). A dose of 25 mg/kg was chosen based on our previous MTD studies. DTIC was used as a positive control. A dose of 60 mg/kg was chosen based on literature (21).

After 31 days of treatment (Fig. 5a), ABI-288 inhibited melanoma tumor growth (TGI value) by

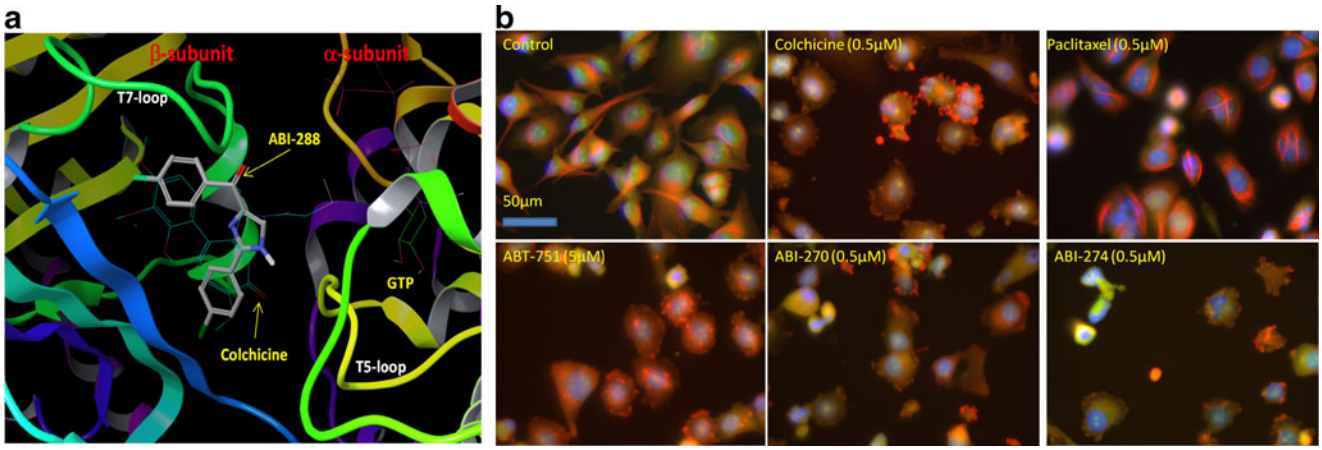

Fig. 3 Molecular modeling and microscopic images showed that ABIs target tubulin in the colchicine binding site. (**a**) Potential binding pose of ABI-288 (stick model) in tubulin crystal structure (1SA0) at the colchicine binding pocket, and it well overlaps with the native ligand (DAMA-colchicine, shown as a wire model). (**b**) Microscopic images of immunofluorescence-labeled microtubules in WM-164 cells showed that microtubule modality was dramatically changed, confirming that ABIs target tubulin and disrupt functional microtubule formation.

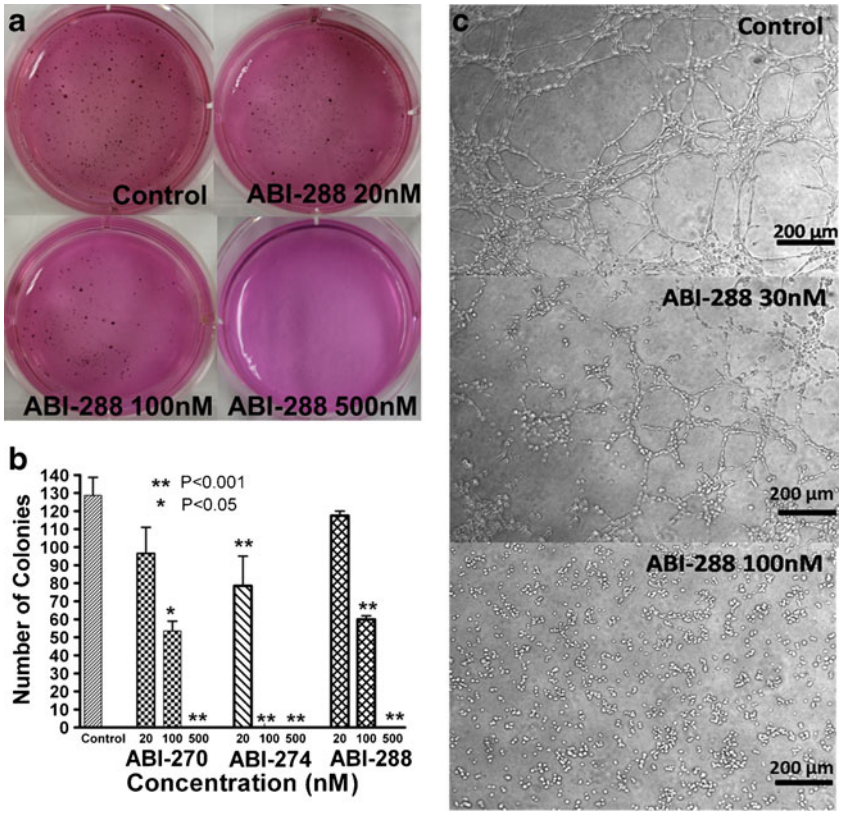

Fig. 4 ABIs inhibited B16-F1 melanoma cell colony formation and HMEC cell capillary network formation in a concentration-dependent manner. (**a**) Representative pictures of control and ABI-288 tested at 20, 100, and 500 nM. The diameter of each well was 35 mm. (**b**) Quantification of assay for each compound. Columns: means of three replicates; bars: SD. (**c**) Representative pictures of HMEC capillary network formation assay on Matrigel. Pictures were taken after 4 h of incubation. Control: 0.01 % DMSO.

69 %, whereas DTIC inhibited growth by 52 %. The repeated measures two-way ANOVA analysis *P* value of ABI-288 treatment *versus* control was 0.006, suggesting that ABI-288 significantly inhibited melanoma tumor growth at 25 mg/kg. Results confirmed that ABI-288 may have comparable activity with DTIC. Body weights of all groups increased slightly throughout the experiment, and all mice showed normal physical activity (Fig. 5b), suggesting that ABI-288 at 25 mg/kg is a well-tolerated, effective dose for SHO mice.

ABIs Inhibited Melanoma Cell Lung Metastasis

Melanoma is highly metastatic, and lung is one of the major target organs for metastasis (28). We used an experimental lung metastasis model established via tail vein injection of melanoma cells to test the efficacy of ABIs in preventing tumor lung metastasis. After 2 weeks of experimental treatment, the average number of detected lung metastasis nodules in control, ABI-270, -274, -288, and DTIC groups were 43, 24, 10, 24, and 26, respectively (Fig. 6a and 6b). There

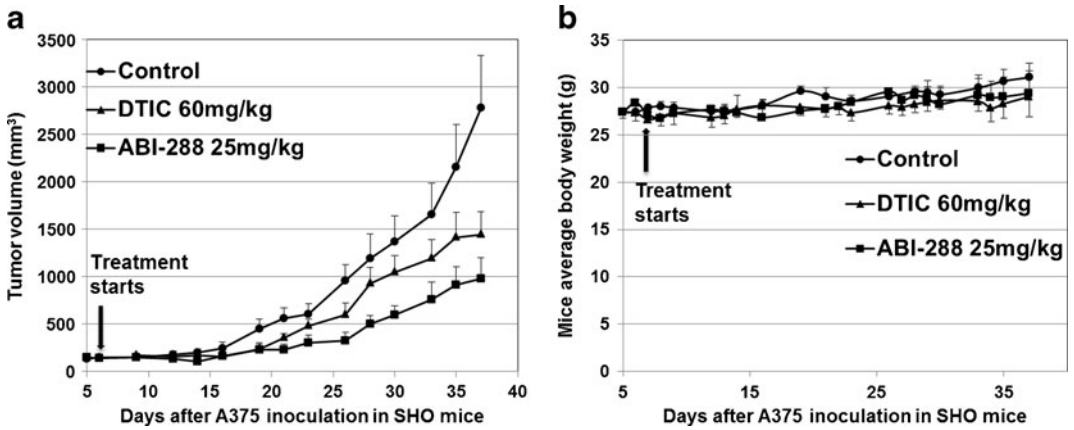

Fig. 5 ABI-288 treatment inhibited xenografted human A375 melanoma tumor growth on SHO mice. (**a**) Tumor growth curves (n=5 per group). Treatment was i.p. injection once daily for 31 days. (**b**) Mouse body weight changes along with time (n=5 per group). Control: vehicle solution only; points: means; bars: SD.

were significant differences among all treated groups ($P<0.0001$ for one-way ANOVA). Dunnett's multiple comparison test using control to compare treatment groups indicated that all treatments were significantly effective in inhibiting lung metastasis ($P<0.01$ for all four comparisons). Dunnett's multiple comparison test using DTIC treatment group to compare all other treatment groups also indicated that ABI-274 treatment was significantly better than DTIC treatment ($P<0.01$). We observed body weight decrease across all groups including control after treatment started (Fig. 6c). But there was no statistical difference between control and other treatment groups (P values of Dunnett's multiple comparison test of control *versus* treatment groups were all larger than 0.05). In the meantime, physical activity of all mice was not obviously affected.

Discussion

Despite the tremendous advances in the understanding of melanoma biology and the recent FDA approvals of new drugs, significant obstacles still exist for finding satisfactory treatments for advanced melanoma. Extending the chemistry research reported earlier for ABIs (9), we performed a series of biological experiments to confirm the mechanisms of action and activities against melanoma for these potent antimitotic agents. We compared the *in vitro* anticancer activity of ABIs with several other antimitotic agents including paclitaxel, vinblastine, colchicine, and ABT-751 (Table I). Paclitaxel and vinblastine are drugs used clinically to target tubulin (29,30). ABT-751 is a clinical candidate developed by Abbott Laboratories and targets the colchicine binding site in tubulin (31). Our experiments showed that ABIs have similar activity with these drugs against melanoma cells *in vitro*.

We next investigated ABIs' effect on MDR cell lines, because drug resistance is a major cause of cancer chemotherapy failure in metastatic melanoma patients. One of the major contributors to MDR is overexpression of ATP-binding cassette (ABC) transporters such as P-gp, MRPs, and BCRP (32). Numerous studies have strongly suggested that these transporters are involved in cancer cell

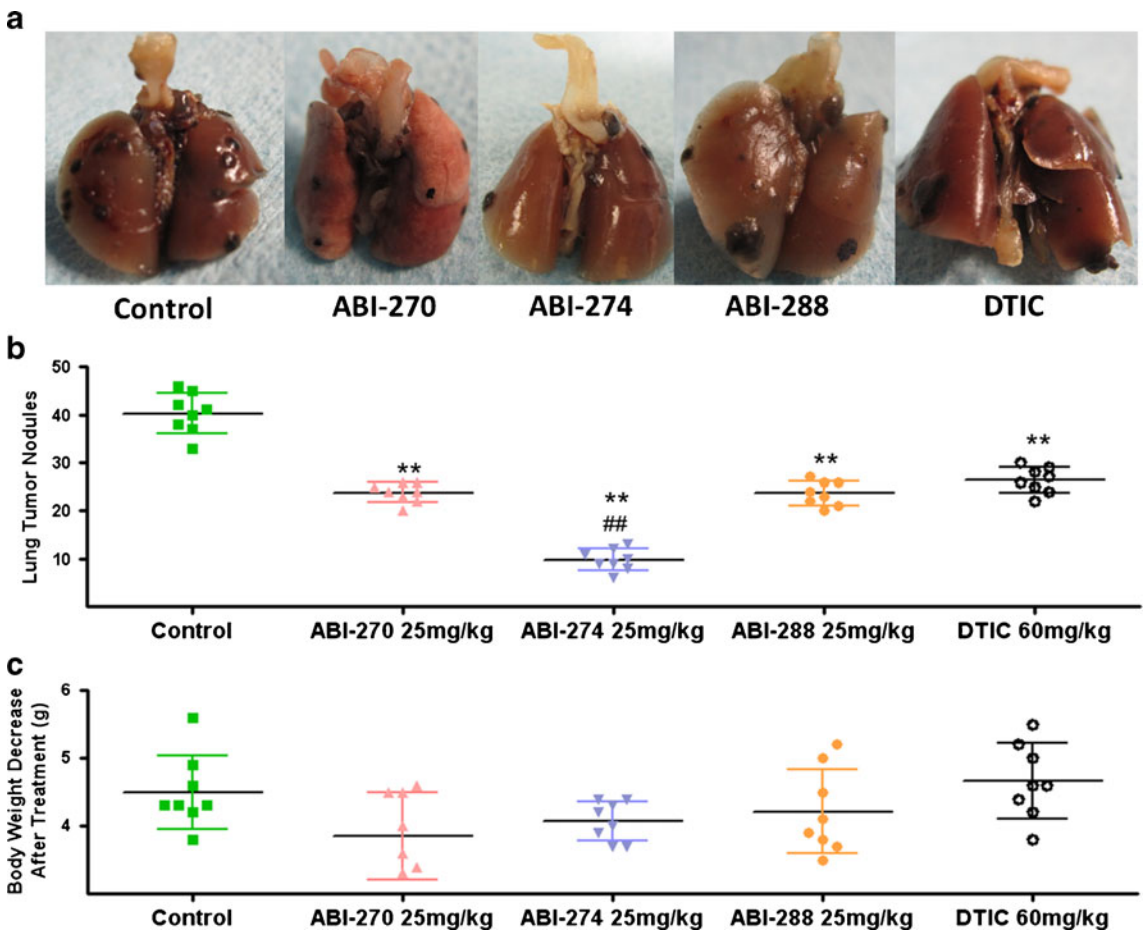

Fig. 6 ABIs and DTIC treatment inhibited B16-F10 melanoma cell metastasis to lungs of C57BL/6 mice after tail vein inoculation. (**a**) Representative photos of lungs with melanoma nodules (black dots) on them ($n=8$ per group). Treatment was i.p. injection 5 days/week for 2 weeks. (**b**) Number of melanoma nodules on each lung. Points: individual nodule number; long line in the middle: mean; short line on the top and bottom: 95 % confidence intervals. (**c**) Mouse body weight changes during experiment. Points: means; bars: SD. Control: vehicle solution only.

migration and invasion of metastatic melanoma (33–35). Tubulin-targeting agents including SMARTs are effective apoptosis inducers (36), but one of the major drawbacks for many existing antitubulin agents (e.g., paclitaxel and vinblastine) is that they are subject to ABC transporter-mediated drug efflux (37). Data presented in Table I indicate that ABIs are effective in overcoming a variety of clinically relevant drug resistance mechanisms at least *in vitro* and strongly support their further preclinical development.

P-gp, also known as MDR1 and ABCB1, is a 170 kDa integral plasma membrane protein that functions as an ATP-dependent drug efflux pump and plays an important role in multi-drug resistance and certain adverse drug-drug interactions. Compounds that interact with P-gp can be identified as stimulators or inhibitors of its ATPase activity. Compounds that are substrates for transport by P-gp typically stimulate its ATPase activity (38). Thus compounds that do not affect ATPase activity normally are likely not substrate for P-gp.

The Pgp-Glo™ Assay detects the effects of a compound on recombinant human P-gp in a cell membrane fraction. The assay relies on the ATP dependence of the light-generating reaction of firefly luciferase. P-gp dependent decreases in luminescence reflect ATP consumption by P-gp; thus the greater the decrease in signal, the higher the P-gp activity. Accordingly, samples containing compounds that stimulate the P-gp ATPase will have significantly lower signals than untreated samples. In our assay, all three ABI compounds were tested at 10, 100, and 1000 nM. None of them significantly lowers luminescence signals compared with vehicle control, indicating that they do not interact with P-gp ATPase and are unlikely to be substrate of P-gp.

Our preliminary studies suggested that ABIs interact with the colchicine binding site in tubulin (9). To clearly define their mode of action, we performed cell cycle analysis, [^{3}H]colchicine competition-binding scintillation proximity assay (SPA), and immunofluorescence assay with melanoma cells. Cell cycle analysis clearly indicated a G2/M phase arrest in melanoma cells, which is typical for antimitotic agents. To pinpoint the possible binding site in tubulin, we tested ABIs' direct effect on tubulin polymerization and measured binding affinity (39). The SPA technology we used in this study requires a close association between the solid-phase scintillant (beads) and the radioligand for a signal to be emitted and subsequently detected. Biotin tubulin was the reagent that brought the [^{3}H]colchicine and the scintillant into close association. The signal amplitude was proportional to the number of colchicine binding sites that were originally occupied by [^{3}H]colchicine. When adding a competitor of [^{3}H]colchicine, e.g., cold (unlabeled) colchicine, to the mixture, the signal amplitude decreased proportionately with the increasing concentration of the competitor. This method is very specific for tubulin colchicine site binding competitors. Our results presented in this report combined with our previously reported tubulin polymerization assay (9) clearly confirmed that ABIs bind to the colchicine site in tubulin to inhibit tubulin polymerization. Immunofluorescence assay with melanoma cells further supported this mode of action.

Angiogenesis is a critical step during cancer progression and metastasis. Several antiangiogenesis agents are in clinical trials for cancers: e.g., cediranib (also called AZD2171, a once-daily oral tyrosine kinase inhibitor that targets vascular endothelial growth factor receptors) for patients with unresectable malignant pleural mesothelioma (40). Some have already shown very promising results. The discovery of ABIs' antiangiogenesis property through this preliminary experiment is exciting, because it opens another venue of cancer progression inhibition. It also suggested to us that ABIs may exert their antimelanoma effect through two mechanisms. Further experiments to confirm this hypothesis and to test whether ABIs inhibit cell movement and invasion ability are ongoing.

The usefulness of any anticancer agents rests in their ability to work *in vivo*. In addition, the major problem for melanoma is its metastasis to sites from the skin, since superficial (early stage) melanoma can be cured by surgical removal. Therefore, it is very important to assess the ability of ABIs to treat melanoma metastasis. The *in vivo* experiments reported here strongly suggest that ABIs are effective in inhibiting not only local melanoma tumor growth but also melanoma lung metastasis. While the experimental lung metastasis model used in this report is not perfect because it bypasses the cell migration process from the primary site to the blood stream, it is a well-established animal model and can provide useful information in assessing the efficacy of new compounds to treat melanoma metastasis. We are currently performing experiments to see whether our MDR cell lines will retain their phenotypes *in vivo*. Once we have confirmed that MDR melanoma cells still possess drug-resistant properties *in vivo*, we will assess the activity of ABIs in tumors grown from MDR cell lines in the future.

CONCLUSION

In this study, we reported *in vitro* activities of ABIs, identified their cellular target, and examined their *in vivo* activity. ABIs are highly potent against melanoma with IC_{50} values in the low nanomolar range, comparable to those of paclitaxel or colchicine. Through a series of data-driven experiments, we further confirmed that the cellular target for ABIs is the colchicine binding site in tubulin. Unlike many of the existing tubulin-targeting drugs, ABIs can effectively overcome P-gp, MRPs, and BCRP-mediated multidrug resistance, which represent some of the major drug resistance mechanisms in melanoma. ABIs inhibited capillary network formation of HMEC cells on Matrigel, indicating that they have strong antiangiogenesis effects. Finally, ABIs showed good *in vivo*

antimelanoma efficacy in one xenograft model and one experimental lung metastasis model. Taking together, these results strongly support the further development of ABIs as potential candidates for improved melanoma treatment.

ACKNOWLEDGMENTS & DISCLOSURES

This work was supported by the NIH/NCI Grant R01CA148706-01A1 to WL with additional partial support from GTx, Inc. (SA, CL and JTD). We thank Dr. Christina Barrett for her help in the colchicine site binding assay, Dr. Feng Zhang for capillary network formation assay, Dr. Bob M. Moore II and Dr. Steven Gurley for helping in taking microtubule images, and Dr. David Armbruster for editorial assistance.

REFERENCES

1. Gray-Schopfer V, Wellbrock C, Marais R. Melanoma biology and new targeted therapy. Nature. 2007;445:851–7.
2. Serrone L, Zeuli M, Sega FM, Cognetti F. Dacarbazine-based chemotherapy for metastatic melanoma: thirty-year experience overview. J Exp Clin Cancer Res. 2000;19:21–34.
3. Mandara M, Nortilli R, Sava T, Cetto GL. Chemotherapy for metastatic melanoma. Expert Rev Anticancer Ther. 2006;6:121–30.
4. Li W, Lu Y, Wang Z, Dalton JT, Miller DD. Synthesis and antiproliferative activity of thiazolidine analogs for melanoma. Bioorg Med Chem Lett. 2007;17:4113–7.
5. Eggermontand AM, Robert C. New drugs in melanoma: it's a whole new world. Eur J Cancer. 2011;47:2150–7.
6. Kahlerand KC, Hauschild A. Treatment and side effect management of CTLA-4 antibody therapy in metastatic melanoma. J Dtsch Dermatol Ges. 2011;9:277–86.
7. Roukos DH. PLX4032 and melanoma: resistance, expectations and uncertainty. Expert Rev Anticancer Ther. 2011;11:325–8.
8. Lu Y, Li CM, Wang Z, Ross 2nd CR, Chen J, Dalton JT, Li W, Miller DD. Discovery of 4-substituted methoxybenzoyl-aryl-thiazole as novel anticancer agents: synthesis, biological evaluation, and structure-activity relationships. J Med Chem. 2009;52:1701–11.
9. Chen J, Wang Z, Li C-M, Lu Y, Vaddadya PK, Meibohma B, Dalton JT, Miller DD, Li W. Discovery of novel 2-aryl-4-benzoyl-imidazoles targeting the colchicines binding site in tubulin as potential anticancer agents. J Med Chem. 2010;53:7414–27.
10. Fox E, Maris JM, Widemann BC, Goodspeed W, Goodwin A, Kromplewski M, Fouts ME, Medina D, Cohn SL, Krivoshik A, Hagey AE, Adamson PC, Balis FM. A phase I study of ABT-751, an orally bioavailable tubulin inhibitor, administered daily for 21 days every 28 days in pediatric patients with solid tumors. Clin Cancer Res. 2008;14:1111–5.
11. Zhang F, Michaelson JE, Moshiach S, Sachs N, Zhao W, Sun Y, Sonnenberg A, Lahti JM, Huang H, Zhang XA. Tetraspanin CD151 maintains vascular stability by balancing the forces of cell adhesion and cytoskeletal tension. Blood. 2011;118:4274–84.
12. Ahn S, Hwang DJ, Barrett CM, Yang J, Duke 3rd CB, Miller DD, Dalton JT. A novel bis-indole destabilizes microtubules and displays potent *in vitro* and *in vivo* antitumor activity in prostate cancer. Cancer Chemother Pharmacol. 2011;67:293–304.
13. Wang Z, Lu Y, Seibel W, Miller DD, Li W. Identifying novel molecular structures for advanced melanoma by ligand-based virtual screening. J Chem Inf Model. 2009;49:1420–7.
14. Chen J, Smith M, Kolinsky K, Adames V, Mehta N, Fritzky L, Rashed M, Wheeldon E, Linn M, Higgins B. Antitumor activity of HER1/EGFR tyrosine kinase inhibitor erlotinib, alone and in combination with CPT-11 (irinotecan) in human colorectal cancer xenograft models. Cancer Chemother Pharmacol. 2007;59:651–9.
15. Bhattacharyya B, Panda D, Gupta S, Banerjee M. Anti-Mitotic Activity of Colchicine and the Structural Basis for Its Interaction with Tubulin. Medi Res Rev. 2008;28:155–83.
16. Zmijewski MA, Li W, Zjawiony JK, Sweatman TW, Chen J, Miller DD, Slominski AT. Photo-conversion of two epimers (20R and 20S) of pregna-5,7-diene-3beta, 17alpha, 20-triol and their bioactivity in melanoma cells. Steroids. 2009;74:218–28.
17. Bazaa A, Pasquier E, Defilles C, Limam I, Kessentini-Zouari R, Kallech-Ziri O, El Battari A, Braguer D, El Ayeb M, Marrakchi N, Luis J. MVL-PLA2, a snake venom phospholipase A2, inhibits angiogenesis through an increase in microtubule dynamics and disorganization of focal adhesions. PLoS One. 2010;5:e10124.
18. Tong YG, Zhang XW, Geng MY, Yue JM, Xin XL, Tian F, Shen X, Tong LJ, Li MH, Zhang C, Li WH, Lin LP, Ding J. Pseudolarix acid B, a new tubulin-binding agent, inhibits angiogenesis by interacting with a novel binding site on tubulin. Mol Pharmacol. 2006;69:1226–33.
19. Guo W, Wu S, Liu J, Fang B. Identification of a small molecule with synthetic lethality for K-ras and protein kinase C iota. Cancer Res. 2008;68:7403–8.
20. Gourdeau H, Leblond L, Hamelin B, Dong K, Ouellet F, Boudreau C, Custeau D, Richard A, Gilbert MJ, Jolivet J. Species differences in troxacitabine pharmacokinetics and pharmacodynamics: implications for clinical development. Clin Cancer Res. 2004;10:7692–702.
21. Povlsenand CO, Jacobsen GK. Chemotherapy of a human malignant melanoma transplanted in the nude mouse. Cancer Res. 1975;35:2790–6.
22. Xu L, Begum S, Hearn JD, Hynes RO. GPR56, an atypical G protein-coupled receptor, binds tissue transglutaminase, TG2, and inhibits melanoma tumor growth and metastasis. Proc Natl Acad Sci U S A. 2006;103:9023–8.
23. Ravelli RB, Gigant B, Curmi PA, Jourdain I, Lachkar S, Sobel A, Knossow M. Insight into tubulin regulation from a complex with colchicine and a stathmin-like domain. Nature. 2004;428:198–202.
24. Salmon SE. Human tumor clonogenic assays: growth conditions and applications. Cancer Genet Cytogenet. 1986;19:21–8.
25. Lau DH, Xue L, Young LJ, Burke PA, Cheung AT. Paclitaxel (Taxol): an inhibitor of angiogenesis in a highly vascularized transgenic breast cancer. Cancer Biother Radiopharm. 1999;14:31–6.
26. Stafford SJ, Schwimer J, Anthony CT, Thomson JL, Wang YZ, Woltering EA. Colchicine and 2-methoxyestradiol Inhibit Human Angiogenesis. J Surg Res. 2005;125:104–8.
27. Li CM, Lu Y, Narayanan R, Miller DD, Dalton JT. Drug metabolism and pharmacokinetics of 4-substituted methoxybenzoyl-aryl-thiazoles. Drug Metab Dispos. 2010;38:2032–9.
28. Kidera Y, Tsubaki M, Yamazoe Y, Shoji K, Nakamura H, Ogaki M, Satou T, Itoh T, Isozaki M, Kaneko J, Tanimori Y, Yanae M, Nishida S. Reduction of lung metastasis, cell invasion, and adhesion in mouse melanoma by statin-induced blockade of the Rho/Rho-associated coiled-coil-containing protein kinase pathway. J Exp Clin Cancer Res. 2010;29:127.
29. Lavelle F, Gueritte-Voegelein F, Guenard D. Taxotere: from yew's needles to clinical practice. Bull Cancer. 1993;80:326–38.
30. Nelson RL. The comparative clinical pharmacology and pharmacokinetics of vindesine, vincristine, and vinblastine in human patients with cancer. Med Pediatr Oncol. 1982;10:115–27.
31. Beerepoot LV, Radema SA, Witteveen EO, Thomas T, Wheeler C, Kempin S, Voest EE. Phase I clinical evaluation of weekly

administration of the novel vascular-targeting agent, ZD6126, in patients with solid tumors. J Clin Oncol. 2006;24:1491–8.
32. Gottesman MM, Fojo T, Bates SE. Multidrug resistance in cancer: role of ATP-dependent transporters. Nat Rev Cancer. 2002;2:48–58.
33. Colone M, Calcabrini A, Toccacieli L, Bozzuto G, Stringaro A, Gentile M, Cianfriglia M, Ciervo A, Caraglia M, Budillon A, Meo G, Arancia G, Molinari A. The multidrug transporter P-glycoprotein: a mediator of melanoma invasion? J Invest Dermatol. 2008;128:957–71.
34. Berger W, Hauptmann E, Elbling L, Vetterlein M, Kokoschka EM, Micksche M. Possible role of the multidrug resistance-associated protein (MRP) in chemoresistance of human melanoma cells. Int J Cancer. 1997;71:108–15.
35. Diestra JE, Scheffer GL, Catala I, Maliepaard M, Schellens JH, Scheper RJ, Germa-Lluch JR, Izquierdo MA. Frequent expression of the multi-drug resistance-associated protein BCRP/MXR/ABCP/ABCG2 in human tumours detected by the BXP-21 monoclonal antibody in paraffin-embedded material. J Pathol. 2002;198:213–9.
36. Li CM, Wang Z, Lu Y, Ahn S, Narayanan R, Kearbey JD, Parke DN, Li W, Miller DD, Dalton JT. Biological activity of 4-substituted methoxybenzoyl-aryl-thiazole: an active microtubule inhibitor. Cancer Res. 2011;71:216–24.
37. Giacomini KM, Huang SM, Tweedie DJ, Benet LZ, Brouwer KL, Chu X, Dahlin A, Evers R, Fischer V, Hillgren KM, Hoffmaster KA, Ishikawa T, Keppler D, Kim RB, Lee CA, Niemi M, Polli JW, Sugiyama Y, Swaan PW, Ware JA, Wright SH, Yee SW, Zamek-Gliszczynski MJ, Zhang L. Membrane transporters in drug development. Nat Rev Drug Discov. 2010;9:215–36.
38. Ambudkar SV, Dey S, Hrycyna CA, Ramachandra M, Pastan I, Gottesman MM. Biochemical, cellular, and pharmacological aspects of the multidrug transporter. Annu Rev Pharmacol Toxicol. 1999;39:361–98.
39. Tahir SK, Kovar P, Rosenberg SH, Ng SC. Rapid colchicine competition-binding scintillation proximity assay using biotin-labeled tubulin. Biotechniques. 2000;29:156–60.
40. Nikolinakosand P, Heymach JV. The tyrosine kinase inhibitor cediranib for non-small cell lung cancer and other thoracic malignancies. J Thorac Oncol. 2008;3:S131–134.